University of BRISTOL

University of Bristol - Explore Bristol Research
General rights

BMJ Open

Deep recurrent reinforced learning model to compare the efficacy of targeted local versus national measures on the spread of COVID-19 in the UK

Tim Dong 🆔 , Umberto Benedetto, Shubhra Sinha, Daniel Fudulu, Arnaldo Dimagli, Jeremy Chan, Massimo Caputo, Gianni Angelini

ABSTRACT

Objectives To prevent the emergence of new waves of COVID-19 caseload and associated mortalities, it is imperative to understand better the efficacy of various control measures on the national and local development of this pandemic in space–time, characterise hotspot regions of high risk, quantify the impact of under-reported measures such as international travel and project the likely effect of control measures in the coming weeks.

Methods We applied a deep recurrent reinforced learning based model to evaluate and predict the spatiotemporal effect of a combination of control measures on COVID-19 cases and mortality at the local authority (LA) and national scale in England, using data from week 5 to 46 of 2020, including an expert curated control measure matrix, official statistics/government data and a secure web dashboard to vary magnitude of control measures.

Results Model predictions of the number of cases and mortality of COVID-19 in the upcoming 5 weeks closely matched the actual values (cases: root mean squared error (RMSE): 700.88, mean absolute error (MAE): 453.05, mean absolute percentage error (MAPE): 0.46, correlation coefficient 0.42; mortality: RMSE 14.91, MAE 10.05, MAPE 0.39, correlation coefficient 0.68). Local lockdown with social distancing (LD_SD) (overall rank 3) was found to be ineffective in preventing outbreak rebound following lockdown easing compared with national lockdown (overall rank 2), based on prediction using simulated control measures. The ranking of the effectiveness of adjunctive measures for LD_SD were found to be consistent across hotspot and non-hotspot regions. Adjunctive measures found to be most effective were international travel and quarantine restrictions.

Conclusions This study highlights the importance of using adjunctive measures in addition to LD_SD following lockdown easing and suggests the potential importance of controlling international travel and applying travel quarantines. Further work is required to assess the effect of variant strains and vaccination measures.

INTRODUCTION

COVID-19 is a highly infectious disease that resulted in a global pandemic in just under a month.[1] This pandemic has caused global disruptions to individuals, businesses and

Strengths and limitations of this study

► The proposed deep recurrent reinforced learning (DRRL) based model takes into account of both relationships of variables across local authorities and across time, using ideas from reinforcement learning to improve predictions.
► While predicting the geographical trend in COVID-19 cases based on the simulation of different measures in the UK at both the national and local levels in the UK has proved challenging, this study has provided a methodology by which useful predictions and simulations can be obtained.
► The Office for National Statistics only released data on UK international travel up to March 2019 at the time of this study, and therefore, this study used the amount of UK tourists in Spain as a reference variable for understanding the effect of international travel on COVID-19 spread.

governments worldwide. The number of cases has continued to rise exponentially, from 80,239 in February 2020 to 69 million as of December 2020.[1] COVID-19 is unlike other historic pandemics in terms of its rapid worldwide spread, a substantial increase in infected and symptomatic people and a rapid development of newly evolving strains. Recent cases of a new variant of COVID-19 have also been found.[2] These problems are being faced worldwide despite global efforts to control this virus.

The spread of COVID-19 can be modelled as a four-stage process: (1) appearance of disease; (2) local transmission; (3) community transmission; and (4) epidemic outbreak.[3] An area can be defined as a liberal zone, a surveillance zone or an infected zone, depending on regional infection patterns, and different levels of restriction measures can be applied.[3] Studies have also focused on the effect of quarantine on COVID-19 spread and have found that it is more effective than

control and combinations with other measures, for example, school closures, travel restrictions and social distancing had a synergistic effect.[4]

Epidemic models developed so far have aimed at understanding the effect of various quarantine factors and mostly applied Newtonian calculus approaches.[5] One study modelled the strictness of lockdown interventions using a contact factor F (ranging from 3 to 8), with three being the strongest and eight being the weakest.[6] In another study, researchers used a COVID-19 decision-making system based on differential formulas and stochastic methods to model transitions between population phase states such as susceptible, exposed, infected, hospitalised, recovered and died. The study was extended to incorporate demographics and social status variables using data from official statistics and the literature.[7] In time-series data analysis and forecasting, deep learning (DL) shows promise. DL models can automatically learn temporal connections and patterns in the data, such as trends and seasonality.[8] Time series and geographical data analysis have been applied to study and inform on optimal energy sector management policies to mitigate the effect of COVID-19.[9] Another study also visualised the geographical distribution of COVID-19 cases.[10] For forecasting worldwide COVID-19 incidence as well as for country-specific and city-specific predictions, one study employed statistics measures to sort the most effective model for medium-term prediction using ARIMA, LSTM, Stacked LSTM (SLSTM) and Prophet models.[11] NAR and FITNET neural networks were combined as an ensemble using a fuzzy weighted approach to predict 10 days ahead of 12 Mexican states.[12] Fuzzy rules have been applied, along with fractal dimension as transformation criteria, to account for linear and non-linear dimensionality in order to forecast the COVID-19 trend.[13] Following this approach, expert knowledge was used to define rules and class memberships with a different set of countries.[14] To model the effect of control measures, a control loop system was used with a novel set of fuzzy logic, with the error between the observed and desired number of infections and the linear fractal dimension of the country as input.[15]

Research gap
From the literature review, we can determine that there are a range of time-series prediction models, each of which outperforms in distinct situations and has its own set of limitations. Although LSTM variants have been used, there have been limited reports of the gated recurrent units (GRUs) DL model. In addition, no DL model results have been mapped to a two-dimensional (2D) choropleth map in order to visualise the effect of control measures. Besides, no application of reinforcement theory has been used for DL analysis. Furthermore, the DL models have not been linked directly to the government website. To add to this, there is a lack of DL models that apply a combination of expert designed matrices and official statistics/government data to incorporate social demographic risk factors for modelling the effects of implementing various restriction measures.

In order to address the limitations of the existing system, the proposed work focuses on the analysis mapping of results from a reinforcement-based DL GRU model (trained with data including longitude and latitude coordinates) onto 2D choropleth maps in order to understand the effectiveness of various control measures. The proposed model is also linked to the Government UK website and an expert-curated matrix to incorporate effects of control measures and social demographic risk factors.[16] A web dashboard for the DL model was built. To the best of our knowledge, this is the first study to apply these techniques to include the examination of hotspot (high incidence) areas in the UK.

Here, the proposed work examines the 2D geographic trend based on simulations of various control measures at both the national and local authority (LA) levels in the UK in order to have a detailed understanding of the factors affecting the spread of COVID-19 at these levels as well as the potential impact of future policy measures. This knowledge would allow the UK government, LAs and individual citizens to make informed decisions about regional policies and personal exposure risks.

METHODS
Patient and public involvement
This research was done without patient and public involvement.

Model development
The proposed model enables predictions of the incidence and mortality related to COVID-19 in the upcoming 5 weeks and simulates the effect of control measures targeting the COVID-19 spread, that is, the number of facilities available for accommodation and food, pubs, retail shops, education, transport and storage, art, entertainment and recreational services, within each LA region. The model also accounts for international migration inflow, internal migration inflow and outflow within the UK, thus simulating control measures that affect travel.

The proposed model is a deep recurrent reinforced learning (DRRL) based model (online supplemental material Part I) named National Coronavirus Global Forecast System (NCGFS) that combines the synergistic properties of GRU[17] and reinforcement deep learning.[18] Like other DL models, GRU has the ability to model non-linear and temporal relationships between and within high dimensions of variables. However, GRU is also expected to be well suited in small dataset scenarios and is computationally more efficient.[19] The reinforcement learning element of NCGFS enables it to adapt to newly inputted data and make more accurate forecasts.

All available LA data were split 80:20 into training and validation data subsets. Data were preprocessed using scaling—subtracting their corresponding mean and dividing by the SD values. Following the completion of

predictions, the prediction outputs are then scaled back to their original scale.

The NCGFS neural network model used an input layer, numerous hidden layers and an output layer. A complex series of non-linear matrix computations are applied to the input data to relate the target output (ie, cases and mortality) and to the other data columns (eg, amount of international migration inflow or internal migration inflow and outflow within UK, number of retail shops, etc). The model is first trained using the existing data subsets provided through a data generator. Each column of the data is assigned a specific weight at each of the nodes in the hidden layers, and these weights are progressively updated to minimise the mean absolute error (MAE) between the predicted and actual values, using the RMSProp optimisation algorithm.[20] Selection for RMSProp is further detailed in online online supplemental material Part I, recurrent optimisation algorithms. During the prediction process, an input data matrix of the same dimension as the training data is then passed into the input layer. The neural network's hidden layers then use the weights learnt during the training process to predict the most likely incidence and mortality based predictor variables from each corresponding week.

The final model consists of two components, model-M (master model) and model-R (reinforced model) that serve different purposes. Model-M accounts for the relationships of variables across different LAs, while model-R provides improved forecasting performance for each individual LA that are selected for analysis. For detailed specifications of model parameters, please see online supplemental material, part I neural network architecture and configuration. This model is particularly apt at generalisation and is capable of forecasting a wide range of LA simultaneously. The model uses model-R to increase forecast performance for the individual LA that are selected for analysis. Model-M is updated with several additional epochs of training data from the selected LA to reinforce and optimise the predictions. Software code is available through https://githubcom/s0810110/Cvd_NCGFS_TrendAnalysis.

Data linkage

The data used to train the deep learning model is based on various datasets that have the potential to influence the trend in the number of COVID-19 cases and mortality at the national and local level (refer to online supplemental materials, part II. A for more details), including domains of deprivation,[21] number of bars and pubs,[22] business size,[23] population estimate (male, female, by age and overall),[24] etc.[25–27] We use the R language and the R software development kit (SDK) for COVID-19, that is, a set of software commands to retrieve data remotely, as published by Public Health England, to automatically extract the latest daily cases and mortality figures for all LA within the UK. Using this approach, we are able to automate and dynamically predict the cases and mortality as new data are generated by GOV.UK. We use R to

convert these data from daily figures into weekly counts and link these data to the data described in online supplemental materials, Part II. A.

Specifically, knowledge from experts in risk modelling is used to curate a matrix containing three indices that together are named the COVID-19 General Policy indices: LockdownScore, QuarantineMeasures[28] and SchoolOpening.[27 29] The main dataset is connected to these index scores based on the weeks each of the associated policies was implemented and the relative effects at each time period.

Furthermore, the number of tourists arriving in Spain from January 2020 to July 2020 were obtained and adjusted by the proportion of UK tourists in Spain from the year 2019. As data on international travel is not readily available for the period affected by COVID-19, the rationale is to use the amount of UK travel to Spain as an indicator for the impact of international travel on the spread of COVID-19,[30 31] since Spain is a frequent UK tourist destination. Our GRU model is trained on the above data and includes the longitude and latitude of each LA as part of the model.[32]

A secured web dashboard was developed that enables users to explore the adjustment effects of risk factors and control measures on the spread of COVID-19 and can be made available on request (http://137.222.198.54:8081/).

While the LA boundaries data are not included in the training process, the main dataset is also linked to these data following forecast generation, so the deep learning model will also provide the prediction of the incidence or mortality in the next 5 weeks in a geographical map view. Furthermore, the model has the capability to toggle the map view by LA or Public Health England regions. These views will be useful for the government to see the future effects of different control measures changes and for the individual citizens to understand their risk of movement within and between local regions in the upcoming future.

For analysis in the map view, the geographical regions from the top to bottom of England is divided into four equidistant slices, which we shall name slice n2, n1, s1 and s2, respectively. These categories will be applied to all other geographical plots hereafter to facilitate discussion. The areas with a higher number of cases are shown in darker colours with 6 grades of severity (I–VI) covering the ranges 0–250 (I); 250–500 (II); 500–750 (III); 750–1000 (IV); 1000–1250 (V); and 1250–1500 (VI). Any number outside of this range is shown in grey and is classed as grade VII.

Model validation

The model is internally validated for the whole of England, whereby the model is trained using all data except for weeks 41–46. The data from this interval are evaluated using root mean squared error (RMSE), mean absolute error (MAE), mean absolute percentage error (MAPE) and correlation coefficient.[11 12] Average ranking of performance metrics were performed as per eqs. 24 and 25.[11]

At the time of this work, only data up to week 46 are available. The risk and control parameters are adjusted within the web dashboard from week 40 onwards to enable predictions to simulate a full/national lockdown (FLD) from week 45 onwards. This is because it is known that a FLD had been applied in the UK from week 45 (00.01 on Thursday, 5 November 2020), and prior to that, local lockdown with social distancing (LD_SD) had been implemented.[33]

During the revision of this work, data for week 51 had become available and was downloaded from GOV.UK to enable external validation of simulated results. This was performed for top 21 hotspots using LD_SD and FLD separately. The same statistic metrics were used as that for internal validation. The following section explains the model simulation process in more details.

Model simulation

Simulations are performed using the final model that is trained using the approach described in the model development section. All data, that is, from week 5 to 46 are included for training this model. The model is used to simulate the effects of numerous different COVID-19 prevention measures on the number of cases at week 51, that is, 5 weeks ahead of the latest available data. The risk and control parameters that model the corresponding measures are set from week 40 onwards to enable predictions to simulate the implementation of various measures from week 45 onwards, rather than FLD, which was what the government actually implemented. The measures simulated are: (A) No lockdown versus LD_SD; (B) LD_SD versus FLD; (C) LD_SD versus LD_SD with international travel −50%; (D) LD_SD versus LD_SD with closing school −50%; (E) LD_SD with travel quarantine 5.5 (see online supplemental material, part II. A., 11) versus LD_SD with full travel quarantine 10; (F) LD_SD with 100% pubs open versus LD_SD with −50% pubs; (G) LD_SD with 100% food and accommodation services open versys LD_SD with −50% food and accommodation services open; (H) LD_SD with −50% retail services open versus LD_SD with 100% retail services open. For details on the implementation of these measures, please refer to online supplemental material, part II. A.

These measures are simulated first for individual LA by selecting a baseline LA with a relatively low case count and comparing the effect of the measures when applied to a LA with a very high number of cases, that is, a hotspot area. The measures are then ranked by order of effectiveness. This is so that the relative effectiveness of each measure can be understood at the local level. Second, the measures are simulated for all the LA in England to visualise the relative effectiveness of each measure at a national level. For the 21 LAs with the highest cases when using a LD_SD measure, the predicted cases counts at week 51 are extracted and plotted to analyse the efficacy of each measure across these nationally 'hard' to tackle areas. This comparison also enabled the ranking of the relative effectiveness of each measure at these hotspots.
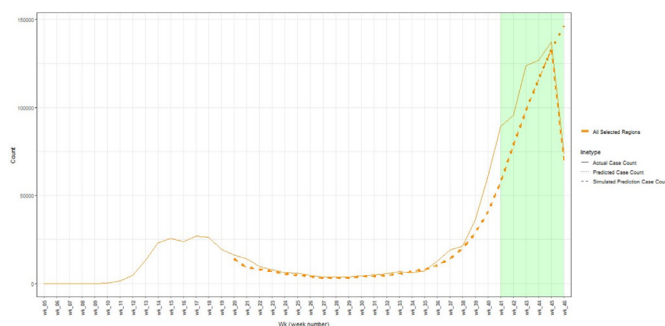

Figure 1 Validation of cases for week 46 with weeks 41–46 excluded from data.
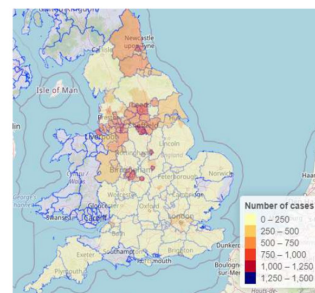
RESULTS

Model validation of predictions against actual results for week 46 showed a good match between the simulation and an actual number of cases across all the LA concerned (figure 1). The model distinguished the LA with high cases from the areas with a low number of cases (figure 2A,B). Furthermore, the model performs especially well for low-grade LA (table 1). The tendency towards better performance in low degree LA, maybe because data from weeks 41 to 46 containing sharp changes in the trend have not been included. Good performance was achieved in terms of RMSE, MAE, MAPE, correlation coefficient and ranking when benchmarked against Devaraj et al[11] and Melin et al[12] (online supplemental tables S2 and S3, part III). FLD simulation performed better than LS_SD in external validation using the top 21 hotspots. Results from
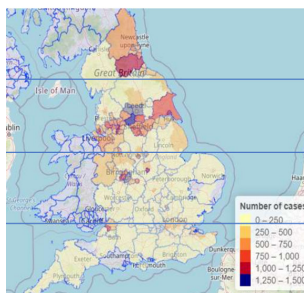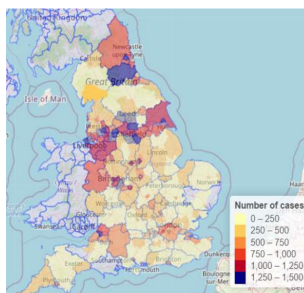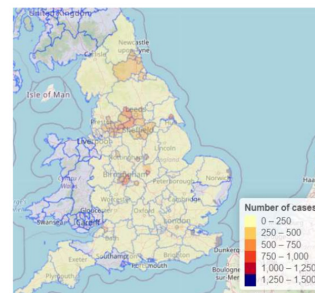

Figure 2 Geographical level of cases for actual and predicted results based on different measures. (A) Exemplifies the use of geographical slices n2, n1, s1 and s2. Additional results are available in online supplemental materials, part II. B. FLD, full/national lockdown; LD_SD, local lockdown with social distancing.

Table 1 Validation model: number of actual and predicted cases and mortalities

Local authority	Number of actual cases for week 46	Cases forecast for week 46	Number of actual mortalities for week 46	Mortality forecast for week 46
Intervention		Full lockdown		
Wolverhampton	438	482	4	5
Gedling	179	196	6	2
Welwyn Hatfield	119	130	0	2
Wiltshire	201	219	1	4
Portsmouth	220	239	0	3
Bromley	217	232	2	3
Stockton-on-Tees	467	498	7	7
Stockport	517	550	13	8
South Kesteven	153	162	6	1
Hammersmith and Fulham	166	175	1	2
Kingston upon Thames	150	158	4	2
Ribble Valley	93	98	4	2
East Cambridgeshire	34	36	1	1
Redcar and Cleveland	380	396	7	4
Sedgemoor	55	57	3	1
Cheshire East	496	514	6	7
Wealden	76	79	1	2
Charnwood	371	382	3	3
South Somerset	72	74	1	1
Southend-on-Sea	137	140	0	3
Chelmsford	110	112	2	2
Rushcliffe	124	126	4	2
Merton	146	148	0	2
Shropshire	426	428	6	6
Harrogate	253	253	1	2
Central Bedfordshire	226	225	5	4
Sutton	155	154	5	3
Oldham	735	732	15	8
Hillingdon	325	323	3	3
Basildon	168	167	4	3
Plymouth	196	192	2	3
Test Valley	59	58	1	1
Walsall	605	590	15	6
Southampton	187	182	0	2
Selby	129	124	2	1
South Holland	105	100	2	1
Chiltern	57	54	0	1
Derbyshire Dales	82	78	1	2
Chichester	58	54	0	1
Barnet	378	354	5	4
Tameside	447	417	18	12
Salford	577	537	17	7
Havant	77	71	1	1
Waverley	97	89	0	1
Nuneaton and Bedworth	247	226	4	3
New Forest	92	84	6	1
Ryedale	67	61	1	1

Continued

Table 1 Continued

Local authority	Number of actual cases for week 46	Cases forecast for week 46	Number of actual mortalities for week 46	Mortality forecast for week 46
Peterborough	224	204	2	4
North Hertfordshire	89	81	1	1
Epping Forest	130	118	2	1

The results show that there is a close match between the actual and predicted number of cases, especially for LA at grade III or below.
Only 50 LAs are displayed. For validation data on all LA, please contact the authors.

simulation of cases and mortality up to week 51, using data from weeks 41 to 46, are further discussed further.

The effects of different measures were first observed at a local level. Southampton was selected as a baseline for observing the effects of measure changes. As Southampton is a grade I LA with a low case number of 187 in week 46, the effects of measure changes were readily perceived with effectiveness ranked from most effective to least effective (online supplemental figure S6, part IV): (b) full lockdown; (c) LD_SD and international travel −50%; (e) LD_SD and 100% quarantine; (d) LD_SD and closing school −50%; and (f) LD_SD and closing pubs −50%. There were negligible differences observed between LD_SD and (g) LD_SD & −50% food and accommodation and (h) LD_SD and −50% retail.

As Leeds was in the highest grade (VII) for both week 46 (actual) and week 51 (predicted), it was selected for observing the effects of different measures on 'hard' to tackle areas. As the number of cases for Leeds was approximately five times higher than Southampton, the effect of measures relative to the number of cases in any week were much smaller in the former than the latter. For Leeds, no difference was observed for predicted cases at week 51 between no lockdown and LD_SD. Full lockdown (online supplemental figure S7b, part IV) was the most effective, followed by LD_SD with a reduction in international travel by 50%, although the effects were much less in proportion to the number of cases than Southampton. There was a negligible impact on the number of cases at week 51 for the remaining measures (online supplemental figure S7e-h).

Figure 2C shows the predicted cases in week 51 using LD_SD. At a national level, it can be seen that there would be a rapid rise in the number of cases, especially in the horizontal 'belt' along the n1 region. In addition, there is at least one LA in each of the other slices n2, s1 and s2 that are expected to rise to grade VI or above. The majority of LA locations elsewhere, which were mostly at grade I in week 46, are expected to rise to grade II or III. The top 21 hotspots at week 51 using LD_SD were selected for subsequent analysis (table 2).

LD_SD was shown (figure 3) to be effective in suppressing the increase in cases for Birmingham (−17%), Bradford (+0.98%), Kirklees (−6.6%) and Leicester (−1.3%). LD_SD was shown to be ineffective for suppressing the increase in cases for the remaining 17 LA, with the highest predicted rises for Wirral (325%),

Stockport (163%), Tameside (188%), Rotherham (158%) and Derby (130%).

LD_SD with −50% international travel was the most effective measure after full lockdown (blue vs brown, figure 4). One hundred per cent quarantine (pink) was the next most effective supplementary measure, with similar effectiveness to international travel −50% except for three LA. Notably, LD_SD with 100% quarantine resulted in higher cases than LD_SD with international travel −50% for Bradford (+9.1%) and Leicester (+7.6%). As an exception, Manchester had −41% fewer cases when using the quarantine measure compared with international travel restrictions.

The supplementary effect of school closing −50% was less than international travel restrictions for all 21 LA, with the number of cases being (+9.2%) higher on average using the former measure. Closing pubs −50% had a similar, although slightly lower level of effectiveness compared with school closing, with a higher number of cases (+2.2%) on average using the former measure compared with the latter. Again, reducing the number of food and accommodation services, −50% had a similar but a slightly lower level of effectiveness compared with pubs closing, with the number of cases (+2.0%) being higher on average using the former measure. In addition, a reduction in the number of retail services −50% resulted in a similar effect to food and accommodation services −50%, with on average a minimal increase in the number of cases (+0.29%) using the former measure. It can be seen that, on average, the ranking of measure effectiveness for the national hotspots are the same as the local baseline, that is, Southampton.

DISCUSSION

Previous studies have evaluated the prediction performances of DL and non-DL based models without 2D choropleth analysis and found that SLSTM outperformed other models because of better hyperparameter tuning and reduction in bias. In addition, it was found that ARIMA outperforms LSTM model.[11] Using the same average ranking metrics, we found that NCGFS (overall rank 1–3) outperformed SLSTM (overall rank 4), ARIMA (overall rank 5) and LSTM (overall rank 6). However, there are several limitations of this comparison: (1) predictions are for different countries; (2) lower mortality rates in England compared with India may bias better ranking towards NCGFS; and (3) comparison does not account for recovered cases. NCGFS also demonstrated

Table 2 Final model: number of actual and predicted cases and mortalities

Local authority (LA)	Number of actual cases for week 46	Number of actual mortalities for week 46	Cases forecast for week 51	Mortality forecast for week 51	Cases forecast for week 51	Mortality forecast for week 51
Intervention	*Full lockdown*		*Local lockdown with social distancing*		*Full lockdown*	
Leeds	1801	17	1881	21	499	17
Sheffield	948	36	1784	32	275	14
Birmingham	1957	35	1627	25	537	17
Wigan	759	34	1554	24	346	10
Manchester	1067	13	1550	20	427	13
Bradford	1534	24	1549	20	722	17
Stockport	517	13	1529	17	218	7
Liverpool	750	29	1509	22	234	8
Rotherham	561	20	1448	22	257	7
Kingston upon Hull	1011	21	1368	18	584	12
Oldham	735	15	1336	17	509	11
Wirral	311	13	1324	19	65	4
Bolton	635	18	1299	17	447	11
Bristol	763	8	1296	14	444	13
Tameside	447	18	1288	20	255	7
County Durham	1161	23	1252	26	377	7
Derby	537	11	1234	15	335	8
Walsall	605	15	1233	21	288	7
Kirklees	1292	25	1207	29	557	14
Leicester	1006	7	993	15	581	11
Sandwell	762	21	969	25	398	10

Results are shown for the top 21 LA with the highest predicted cases observed at week 51 using LD_SD.
LD_SD, local lockdown with social distancing.

good performance in terms of case prediction when benchmarked against Modular Neural Network with Fuzzy (MNNF) in terms of RMSE (700.88 vs 1554.03).[12] While a few studies have analysed 2D geospatial predictions, for example, by converting to heatmaps,[34] and considered hotpot regions, these have mainly been using either modified regression or differential equation techniques rather than DL-based techniques.[10 35 36] Although interactive dashboards have been developed for tracking COVID-19,[37] these typically do not enable prediction through simulation of control measures. Furthermore,

although reinforcement learning has been applied, it has not typically been combined with 2D map analysis or lack external validation.[38 39] In this article, we demonstrate the use of a reinforcement-based DL GRU model with 2D choropleth maps to analyse spatial representation of results in order to rank the efficacy of various control measures. The proposed model is embedded in an interactive dashboard linked to the Government UK website and an expert-curated matrix to incorporate effects of control measures and social demographic risk factors. This combination of techniques has not yet been
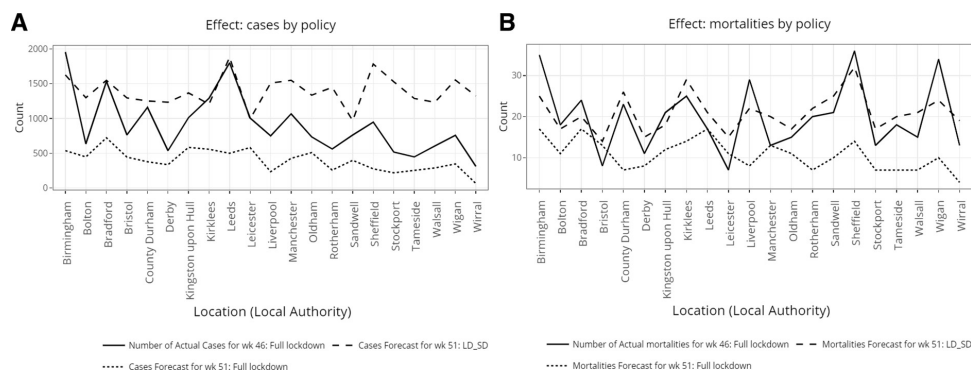

Figure 3 For the top 21 LA with the highest predicted cases observed at week 51 using LD_SD, plots were generated to compare the effects of full lockdown against LD_SD in terms of cases (A) and mortalities (B). LA, local authority; LD_SD, local lockdown with social distancing.
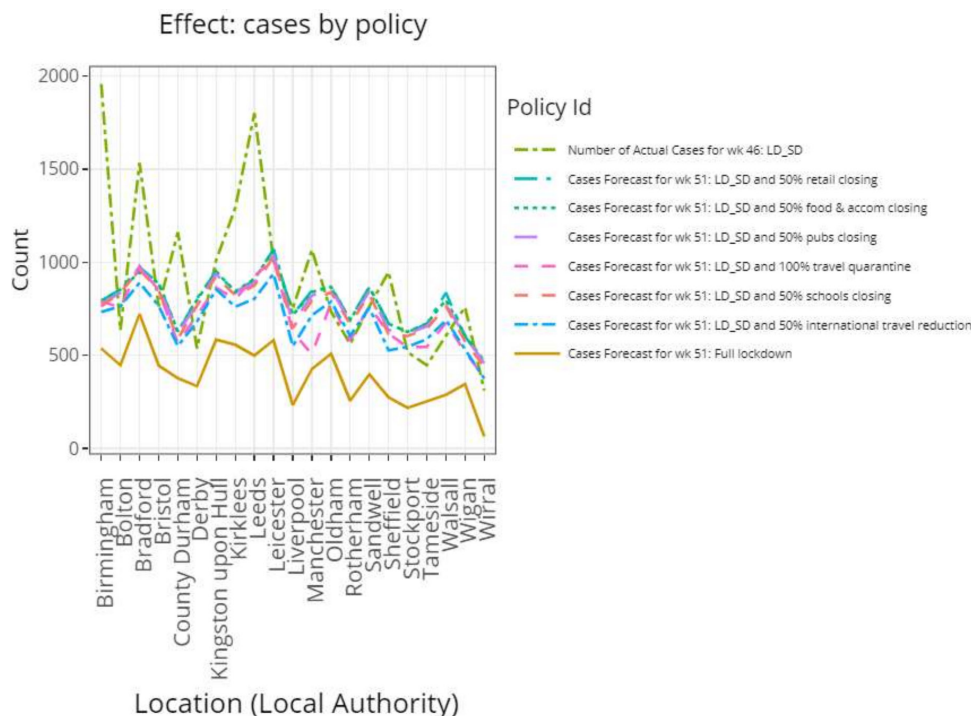
Figure 4 For the top 21 LA with the highest predicted cases observed at week 51 using LD_SD, a plot is generated to compare the effect on the number of cases using a combination of LD_SD with other 'supplementary' measures. LA, local authority; LD_SD, local lockdown with social distancing

widely used, and it provides a number of advantages over each individual formulation alone. The NCGFS model can be used to make inferences into the effectiveness of different measures at both the national and local levels. The model suggests that there is variation in the effect of each measure across different regions. Notably, our results indicate that the protective effects of lockdown measures benefit some local authorities more than others (online supplemental material fig S6 and S7, part IV) and that local lockdown with social distancing is ineffective compared with national lockdown in suppressing the increase in cases for most of the LA areas. That is, if the government had kept the same local lockdown with social distancing policies, which they had implemented from week 40 onwards rather than switching to a national lockdown policy at week 45, then we would have seen a rapid rise in cases nin the n1 belt region and in areas such as County Durham (n2), Bristol (s2) and Birmingham (s1), as well as in many other areas across England.

Local lockdown with social distancing and without additional measures may be inefficient in stopping rapid rise of hotpot regions due to the geographical properties of hotspot regions. Hotspots along the middle of the n1 geographical slice constitute a tight cluster of large metropolitan cities. The high number of cases may be partly attributed to the high number of services such as pubs and schools available and the amount of travel in these areas. We expect that this effect could possibly be enhanced by the fact that the n1 slice contains a large number of LA areas with many boundary links to other hotspots, which agrees with another study that highlighted influences of

neighbouring small areas and found continuous bands of hotspot regions.[36]

Since the government is only able to impose a national lockdown for a limited period, follow-up measures should incorporate LD_SD with additional measures as LD_SD alone is likely not to be sufficient. The actual FLD had lasted only up to 2 December 2020 (week 49), after which LD_SD was implemented by the government. The UK Government had implemented LD_SD for 2 weeks in between week 49 and week 51. As a substantially larger proportion of weeks between week 45 and week 51 were implemented using FLD rather than LD_SD, we found the FLD simulation (overall rank 2) better predicted actual results than LD_SD (overall rank 3) as expected. Trend and 2D map analysis showed that introduction of additional measures on top of local lockdown with social distancing can help to suppress the increase of or even decrease the number of cases in national hotspots as well as local areas where cases are not very high. Our model shows that the ranking of the average effectiveness of each supplementary measure is consistent across the national hotspots and local baseline, and this ranking can be used to prioritise those interventions according to an order of effectiveness. Nonetheless, it was also observed that specific measures are more effective for some LA compared with others. In these cases, it is necessary to adjust the priorities of the measures implemented accordingly.

The model has highlighted the importance of reducing the amount of international travel, the number of open schools and pubs as well as the implementation of travel

quarantine procedures in controlling the spread of COVID-19 over other measures, such as reducing the number of food and accommodation and retail services, which seemed less relevant on the virus spread (figure 4 and online supplemental figure S6). Our finding of the usefulness of restricting international travel and applying travel quarantine is in contrast with another study, which found that quarantine of travel from endemic countries was not effective.[4] One explanation for international travel being more impactful than travel quarantine is that while travel quarantine provides the government with some control over which countries to enforce a 14-day self-isolation on travellers' return, it provides little control over the activities of travelling individuals once they arrive at their destinations as well as the level of preventative health measures at those destinations. Furthermore, the individuals who travel are more likely to encounter places of gathering while abroad. In addition, even with COVID-19 testing in place, the journey from the airport back to the home of the traveller allows an increased opportunity of spreading the virus, particularly if public transport such as taxis or buses are used.[4 8] Therefore, these measures are not as direct as limiting the amount of international travel.

While closing schools were not as effective as international travel and quarantine restrictions, we found this measure to be more effective than closing pubs. One potential explanation for this is that schools are more crowded places and are subject to a more frequent number of close contact scenarios in comparison with the pub. The view that schools contribute to the spread of COVID-19 has been supported by the literature.[40 41] While the virus may pose a low risk of mortality to the children themselves, these frequently asymptomatic carriers can also lead to the spread of the virus to their households, teachers and communities.

The reason why minimal effects were found for food and accommodation and retail restrictions may be because in these sectors, people generally associate with others that they are closely associated with. For example, families are more likely to sit with each other in restaurants or walk together when shopping rather than with people they are less familiar with. This is not the case in pubs as anyone from the communal area can be present.

It is unexpected that in the s2 slice that Bristol has higher predicted cases than the LA in the London area as one would have thought the latter comprising a total population of 9 million (2019) and a high traffic volume owing to its large underground network system would result in much higher case numbers. We expect that this may be because the London region LA generally has less health and disability deprivation (deciles: Wandworth: 7; Barnet: 8.9; Brent: 7.3; and Waltham Forest: 6.1) compared with Bristol (decile: 4.4). This is supported by the findings that suggest that existing comorbidities are associated with an increased likelihood of COVID-19 hospital admission.[42]

In light of evidence given by the comparison between the LA within the London region and Bristol, we expect the effect of LA boundary connections to be adjusted by the degree of health and disability deprivation. Indeed, we found that regions with a high number of cases along the horizontal 'belt' in the n1 region had a high degree of health and disability deprivation (decile: Manchester: 1.9; Leeds: 4.1; Bradford: 3.3; Liverpool: 1.8; Sheffield: 3.9; and Wigan: 3.4). Another study reports a similar result.[36] This also applies to County Durham (n2), which has a high degree of health and disability deprivation (decile: 2.9) and was seen to have a significant increase in cases at week 51 using a LD_SD measure.

One limitation of our study is that for simulated week 51, there was an LA in Kent that was coloured grey on the map but were, in fact, reporting negative values. A future improvement would be to transform or limit the prediction outputs to retain meaningful information while preventing negative values. Nonetheless, the result is interesting and giving the LA a grade of VII may still be valid, since the highly infectious Kent variant emerged in week 39 (20 September).[43] The present study has not specifically dealt with the modelling of variants. In addition, vaccination effects could not be accounted for as these were only beginning to be rolled out (2 December 2, week 49) at the point of this study.[44] While a variety of data sources have been used, this study has not analysed the effect of in-hospital admission or clinical comorbidity. These are issues that deserve to be further explored. Future work could be done to compare the current model against those found in similar studies, for example, ARIMA, LSTM, SLSTM and Prophet,[11] Bayesian hierarchical space–time SEIR model,[36] NAR and FITNET neural networks, using the same dataset.[12] Furthermore, a Hybrid Q-learning based algorithm could be used whereby these models represent potential actions to update the Q cumulative reward matrix.[39] While the current model takes a risk factor matrix as one of its inputs and this was built with expert input, a fuzzy logic approach with functionally modelled inputs and outputs was not used.[15] Incorporating such methods could enhance the interpretability of the risk factor matrix.

CONCLUSION

This study highlights the importance of simulating the effects of various control measures using map and non-map-based analyses to prioritise COVID-19 preventative measures. This was demonstrated for both local hotspot zones and on a nationwide scale. Furthermore, at the LA level, we demonstrated the utility of geographical slicing for comparative analysis of interventional effects across time periods and thereby can also allow governments to assess the optimal measures to apply. It is advisable to assess the effectiveness of lockdown with social distancing alone against that when combined with other adjunctive measures and implement periodic monitoring at both trend and map dimensions to reduce the risk of outbreak rebound following lockdown easing. Lastly, this study highlights the importance of controlling international

travel, and this should be further explored with the comparative analysis of effectiveness against newly developed vaccine measures.

ORCID iD
Tim Dong http://orcid.org/0000-0003-1953-0063

REFERENCES

1 Statista. COVID-19 cases worldwide by day. Available: https://www.statista.com/statistics/1103040/cumulative-coronavirus-covid19-cases-number-worldwide-by-day/ [Accessed 11 Dec 2020].
2 Dyer O. Covid-19: Denmark to kill 17 million minks over mutation that could undermine vaccine effort. *BMJ* 2020;371:m4338.
3 Elavarasan RM, Pugazhendhi R, Shafiullah GM, et al. A hover view over effectual approaches on pandemic management for sustainable cities - The endowment of prospective technologies with revitalization strategies. *Sustain Cities Soc* 2021;68:102789.
4 Kumaravel SK, Subramani RK, Jayaraj Sivakumar TK, et al. Investigation on the impacts of COVID-19 quarantine on Society and environment: preventive measures and supportive technologies. *3 Biotech* 2020;10:393.
5 Varotsos CA, Krapivin VF. A new model for the spread of COVID-19 and the improvement of safety. *Saf Sci* 2020;132:104962.
6 Sun T, Wang Y. Modeling COVID-19 epidemic in Heilongjiang Province, China. *Chaos Solitons Fractals* 2020;138:109949.
7 Varotsos CA, Krapivin VF, Xue Y. Diagnostic model for the society safety under COVID-19 pandemic conditions. *Saf Sci* 2021;136:105164.
8 Madurai Elavarasan R, Pugazhendhi R. Restructured society and environment: a review on potential technological strategies to control the COVID-19 pandemic. *Sci Total Environ* 2020;725:138858.
9 Madurai Elavarasan R, Shafiullah GM, Raju K, et al. COVID-19: Impact analysis and recommendations for power sector operation. *Appl Energy* 2020;279:115739.
10 Melin P, Monica JC, Sanchez D, et al. Analysis of spatial spread relationships of coronavirus (COVID-19) pandemic in the world using self organizing maps. *Chaos Solitons Fractals* 2020;138:109917.
11 Devaraj J, Madurai Elavarasan R, Pugazhendhi R, et al. Forecasting of COVID-19 cases using deep learning models: is it reliable and practically significant? *Results Phys* 2021;21:103817.
12 Melin P, Monica JC, Sanchez D, et al. Multiple ensemble neural network models with fuzzy response aggregation for predicting COVID-19 time series: the case of Mexico. *Health Care* 2020;8:181.
13 Castillo O, Melin P. Forecasting of COVID-19 time series for countries in the world based on a hybrid approach combining the fractal dimension and fuzzy logic. *Chaos Solitons Fractals* 2020;140:110242.
14 Castillo O, Melin P. A novel method for a COVID-19 classification of countries based on an intelligent fuzzy fractal approach. *Healthcare* 2021;9:196.
15 Castillo O, Melin P. A new fuzzy fractal control approach of non-linear dynamic systems: the case of controlling the COVID-19 pandemics. *Chaos Solitons Fractals* 2021;151:111250.
16 Benedetto U, Dimagli A, Gibbison B, et al. Disparity in clinical outcomes after cardiac surgery between private and public (NHS) payers in England. *Lancet Reg Health – Eur* 2021;1:100003.
17 Cho K, van Merrienboer B, Bahdanau D. On the properties of neural machine translation: Encoder-Decoder approaches. *ArXiv*.
18 Mnih V, Kavukcuoglu K, Silver D, et al. Human-level control through deep reinforcement learning. *Nature* 2015;518:529–33.
19 Chung J, Gulcehre C, Cho K. Empirical evaluation of gated recurrent neural networks on sequence modeling. ArXiv14123555 Cs. Available: http://arxiv.org/abs/1412.3555 [Accessed 11 Nov 2021].
20 Zou F, Shen L, Jie Z. A Sufficient Condition for Convergences of Adam and RMSProp. In: *2019 IEEE/CVF conference on computer vision and pattern recognition*. Long Beach, CA, USA: IEEE, 2019: 11119–27.
21 GOV.UK. English indices of deprivation, 2019. Available: https://www.gov.uk/government/statistics/english-indices-of-deprivation-2019 [Accessed 2 Dec 2021].
22 Office for National Statistics. Public houses and bars by local authority. Available: https://www.ons.gov.uk/businessindustryandtrade/business/activitysizeandlocation/datasets/publichousesandbarsbylocalauthority [Accessed 2 Dec 2021].
23 Office for National Statistics. UK business: activity, size and location. Available: https://www.ons.gov.uk/businessindustryandtrade/business/activitysizeandlocation/datasets/ukbusinessactivitysizeandlocation [Accessed 2 Dec 2021].
24 Office for National Statistics. Estimates of the population for the UK, England and Wales, Scotland and Northern Ireland. Available: https://www.ons.gov.uk/peoplepopulationandcommunity/populationandmigration/populationestimates/datasets/populationestimatesforukenglandandwalesscotlandandnorthernireland [Accessed 2 Dec 2021].
25 Boundaries UK BUC. Local authority districts, 2019. Available: https://geoportal.statistics.gov.uk/datasets/local-authority-districts-december-2019-boundaries-uk-buc [Accessed 2 Dec 2021].
26 Lookup in England. Local authority district to public health England centre to public health England region, 2019. Available: https://geoportal.statistics.gov.uk/datasets/local-authority-district-to-public-health-england-centre-to-public-health-england-region-december-2019-lookup-in-england [Accessed 2 Dec 2021].
27 GOV.UK. Actions for schools during the coronavirus outbreak. Available: https://www.gov.uk/government/publications/actions-for-schools-during-the-coronavirus-outbreak [Accessed 2 Dec 2021].
28 The UK's coronavirus timeline. Week UK. Available: https://www.theweek.co.uk/107044/uk-coronavirus-timeline [Accessed 2 Dec 2021].
29 BBC News. Coronavirus: UK schools, colleges and nurseries to close from Friday, 2020. Available: https://www.bbc.com/news/uk-51952314 [Accessed 2 Dec 2021].
30 Statista. Monthly tourist arrivals in Spain 2020. Available: https://www.statista.com/statistics/1130775/number-of-monthly-arrivals-short-stay-accommodation-in-spain/ [Accessed 2 Dec 2021].

31 Statista. Spain: number of tourists by country. Available: https://www.statista.com/statistics/447683/foreign-tourists-visiting-spain-by-country-of-residence/ [Accessed 2 Dec 2021].

32 Public Health England Centres. Ultra generalised clipped boundaries in England, 2016. Available: https://geoportal.statistics.gov.uk/datasets/public-health-england-centres-december-2016-ultra-generalised-clipped-boundaries-in-england [Accessed 2 Dec 2021].

33 Inst. Gov. Timeline of UK government coronavirus lockdowns, 2021. Available: https://www.instituteforgovernment.org.uk/charts/uk-government-coronavirus-lockdowns [Accessed 23 Nov 2021].

34 Khan SD, Alarabi L, Basalamah S. Toward smart Lockdown: a novel approach for COVID-19 hotspots prediction using a deep hybrid neural network. *Computers* 2020;9:99.

35 Islam A, Sayeed MA, Rahman MK, *et al*. Geospatial dynamics of COVID-19 clusters and hotspots in Bangladesh. *Transbound Emerg Dis* 2021;68:3643–57.

36 Sartorius B, Lawson AB, Pullan RL. Modelling and predicting the spatio-temporal spread of COVID-19, associated deaths and impact of key risk factors in England. *Sci Rep* 2021;11:5378.

37 Dong E, Du H, Gardner L. An interactive web-based dashboard to track COVID-19 in real time. *Lancet Infect Dis* 2020;20:533–4.

38 Kumar RL, Khan F, Din S, *et al*. Recurrent neural network and reinforcement learning model for COVID-19 prediction. *Front Public Health* 2021;9:1437.

39 Khalilpourazari S, Hashemi Doulabi H. Designing a hybrid reinforcement learning based algorithm with application in prediction of the COVID-19 pandemic in Quebec. *Ann Oper Res* 2021:1–45.

40 Sheikh A, Sheikh A, Sheikh Z, *et al*. Reopening schools after the COVID-19 lockdown. *J Glob Health* 2020;10.

41 Stein-Zamir C, Abramson N, Shoob H, *et al*. A large COVID-19 outbreak in a high school 10 days after schools' reopening, Israel, May 2020. *Eurosurveillance* 2020;25:2001352.

42 Price-Haywood EG, Burton J, Fort D, *et al*. Hospitalization and mortality among black patients and white patients with Covid-19. *N Engl J Med* 2020;382:2534–43.

43 Mahase E. Covid-19: what have we learnt about the new variant in the UK? *BMJ* 2020;371:m4944.

44 Inst. Gov. Coronavirus vaccine rollout, 2021. Available: https://www.instituteforgovernment.org.uk/explainers/coronavirus-vaccine-rollout [Accessed 26 Nov 2021].

Supplementary Materials: A Deep Recurrent Reinforced Learning model to compare the efficacy of targeted local vs national measures on the spread of COVID-19 in the UK

Tim Dong (0000-0003-1953-0063), Umberto Benedetto (0000-0002-7074-7949), Shubhra Sinha, Daniel Fudulu, Arnaldo Dimagli, Jeremy Chan, Massimo Caputo, Gianni Angelini

Part I.

GRU Gated Recurrent Units Model

We have chosen a Recurrent Neuro Network (RNN) category of model because of the ability of this type of model to model not only non-linear relationships between high dimension of variables, but also because of its ability to model temporal relationships within any of the variables considered. As figure S1. shows, the RNN model consists of cells is analogous to each unit of the traditional neuro network. Whilst traditional neuro network models accumulate weights W_i (input to hidden layer) and W_h (hidden to hidden layer), they do not calculate any recurrent weights W_r that represent temporal relationships of each variable in the dataset. This recurrent type of weight is present in RNN models and hence is desirable for modelling a time dependent COVID-19 dataset.
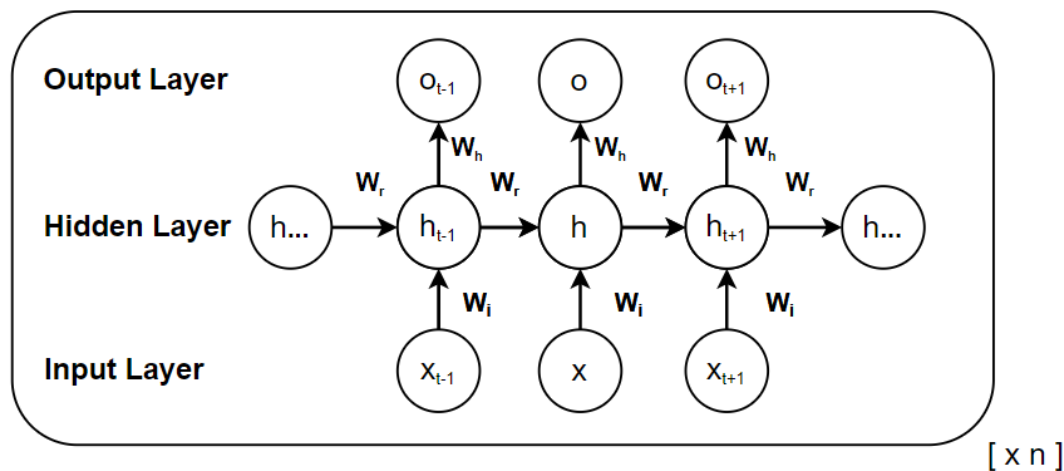
Figure S1. An RNN cell

GRU is a specific type of Recurrent Neuro Network (RNN) that incorporates long term memory and effectively deals with the vanishing gradient and gradient explosion problems that have affected various other categories of RNN. The GRU model was also selected because of its ease to optimise and its low computational cost in comparison to the LSTM model.

Unlike the LSTM model, which uses four gates, the GRU model uses only a single decision gate that controls both the update and reset of weights. The update gate is similar to an OR gate in electronics that either retains the state at the previous step h_{t-1} or updates the previous state based on variable values X_t provided at the current step. The reset gate is much like a resistor in that it controls that size of the effect from previous step that contributes to the current step.

Figure S2. A GRU cell
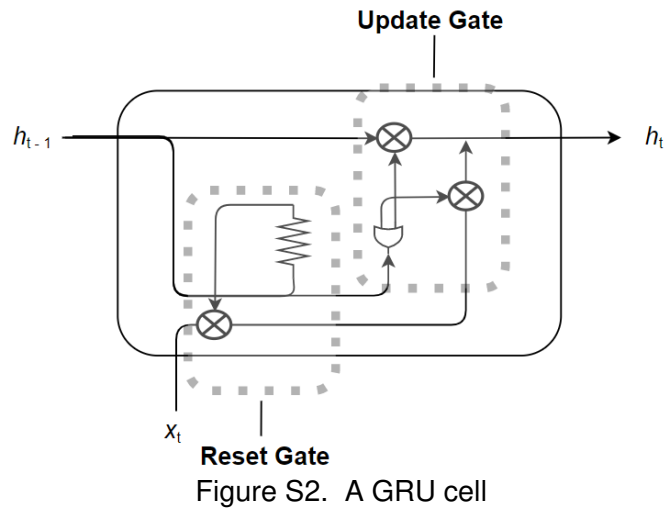
The above diagram above provides an intuitive understanding into the processes that occur within a cell or node of a GRU model. The specific mathematical equation of the GRU model is given below:

$$h_t^i = z_t^i.h_{t-1}^i + \left(1 - z_t^i\right) tanh\left[b^i + \sum_j W_I^{i,j} x_t^j + \sum_j W_R^{i,j} r_{t-1}^j h_{t-1}^j\right]$$

$$z_t^i = \sigma\left(b_z^i + \sum_j W_z^{i,j} x_t^j + \sum_j W_z^{i,j} h_{t-1}^j\right)$$

$$r_t^j = \sigma\left(b_r^i + \sum_j W_r^{i,j} x_t^j + \sum_j W_r^{i,j} h_{t-1}^j\right)$$

where z represents for the update gate and r represents the reset gate, W_I are the weights from the input to hidden layer, W_R are the weights from the recurrent weights, b is the bias, σ and tanh are the sigmoid and tanh activation functions respectively, X_t are the inputs at time t and h_{t-1} was the input from previous time step.

Deep Reinforcement Learning

Deep reinforcement learning is the application of reinforcement learning to neuro networks. The application of this approach has been exemplified in the field of computer gaming.[1] Essentially, the approach involves an agent that represents the computer system, which performs an action in the environment that it interacts with.

The environment is changed following the action and a reward is provided to the agent such that the action it selects from a list of actions or policy π is optimised in any subsequent interactions with the environment.

Here, we present a technique whereby the NCGFS model represents the agent. It is initially presented with a set of observations O_t from the national environment, s. Each individual observation has the property o $\in$ A, where A is the set of all the LA. Rather than using the traditional reward variable r, we use L_t to represent the loss at the initial training phase t of the deep learning model, i.e. at the generation point of model-M. Subsequently, when the agent is presented with the input observations O_{t+1} that belongs to a single local authority, s_{t+1} from the set A, it uses the action or in this case forecast from the list of potential forecasts that previously minimised the L_t for O_t to make the forecast f_t for O_{t+1}. This induces a loss L_{t+1} that is used to update the NCGFS model's policy decisions for the actual prediction of O_{t+1} as f_{t+1}. The resulting model is termed model-R.
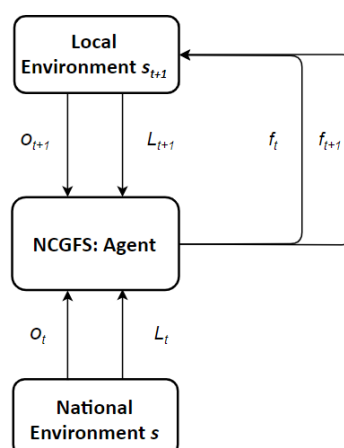
Figure S3. illustration of the Deep Reinforcement Learning aspect of NCGFS at the local authority level.

The following equation shows how NCGFS uses deep reinforcement learning to minimise the Loss L for a given environment s to produce an optimal forecast from the probabilistic distribution of forecasts $\pi = P(f|s)$.

$$Q^*(s, f) = \min_{\pi} \frac{1}{n} \left(\sum_{i}^{n} \gamma^i L_{t+i} \mid s_t = s, f_t = f, \pi \right)$$

Recurrent Optimization Algorithms

RMSProp was found empirically to be the optimal algorithm for optimization of the proposed model. Adam was not selected as the dataset size was small and the algorithm did not converge.

Table S1. Adapted summary of optimization algorithms considered.[2]

Method	Properties	Advantages	Disadvantages
GD	Solve the optimal value along the direction of the gradient descent. The method converges at a linear rate.	The solution is global optimal when the objective function is convex.	In each parameter update, gradients of total samples need to be calculated, so the calculation cost is high.
SGD	The update parameters are calculated using a randomly sampled mini-batch. The method converges at a sublinear rate.	The calculation time for each update does not depend on the total number of training samples, and a lot of calculation cost is saved.	It is difficult to choose an appropriate learning rate, and using the same learning rate for all parameters is not appropriate. The solution may be trapped at the saddle point in some cases.
AdaGrad	The learning rate is adaptively adjusted according to the sum of the squares of all historical gradients.	In the early stage of training, the cumulative gradient is smaller, the learning rate is larger, and learning speed is faster. The method is suitable for dealing with sparse gradient problems. The learning rate of each parameter adjusts adaptively	As the training time increases, the accumulated gradient will become larger and larger, making the learning rate tend to zero, resulting in ineffective parameter updates. A manual learning rate is still needed. It is not suitable for

			dealing with non-convex problems
AdaDelta/ RMSProp	Change the way of total gradient accumulation to exponential moving average.	Improve the ineffective learning problem in the late stage of AdaGrad. It is suitable for optimizing non-stationary and non-convex problems.	In the late training stage, the update process may be repeated around the local minimum.
Adam	Combine the adaptive methods and the momentum method. Use the first-order moment estimation and the second order moment estimation of the gradient to dynamically adjust the learning rate of each parameter. Add the bias correction.	The gradient descent process is relatively stable. It is suitable for most non-convex optimization problems with large data sets and high dimensional space.	The method may not converge in some cases.

Neural Network architecture and configuration
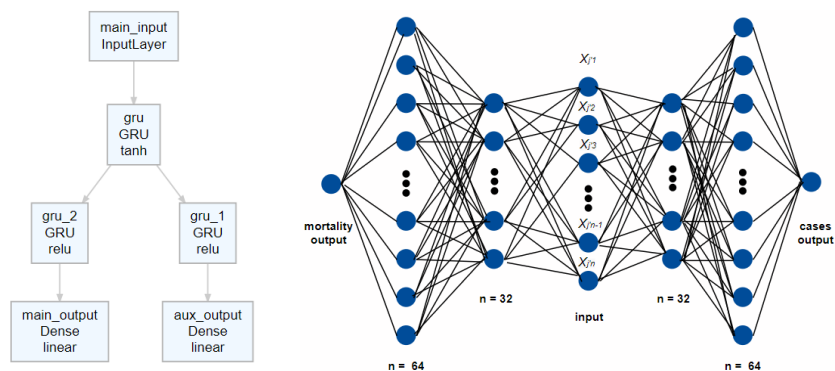
Figure S4.1 NCGFS model architecture. Note, the two layers on either side of the input layer have been depicted in this manner to facilitate representation but represent the same layer.

The model is comprised of symmetrical neuro network that consists of six layers.

The input layer accepts a data matrix in the dimension of $[d \quad \tau \quad n]$, where $d = 136$ is the number of variables, $\tau = 2$ is the number of time steps in the recurrent direction along the hidden layer, n is the number of samples taken from the observation. The

Supplemental material

BMJ Publishing Group Limited (BMJ) disclaims all liability and responsibility arising from any reliance placed on this supplemental material which has been supplied by the author(s)

BMJ Open

layer immediately right of the input layer is named gru and consists of 32 GRU cells or units. The next layer to the right is name gru_2 and consists of 64 GRU cells. The output from this layer uses the ReLU activation function as this has been demonstrated to be effective for the convergence of neuro networks. This is followed by a dense output layer named main_output, consisting of one unit on the right. This layer provides the prediction output for the number of COVID-19 cases five weeks ahead of the corresponding weeks in the input data.

The layer immediately left of the input layer is in fact the same layer as that to the right of input layer i.e. named gru. The next layer to the left is a named gru_1 and consists of 64 GRU cells. This is followed by a dense output layer named aux_output for prediction the number of mortalities five weeks ahead of the corresponding weeks in the input data.

We have empirically found that this combination of depth and width is efficient for the minimising the loss of the learning problem at hand.

Model-M was trained using four iterations of 500 epochs (with 6 steps per training epoch and 1 step per validation epoch) using early stop to stop training once validation loss has stopped decreasing with a difference of 0.001 and patience of 200. With the four iterations of training, NCGFS model-M had achieved a performance validation loss of 0.17456 per epoch consisting of the sum of validation loss for both cases and mortality.

Part II. A

1. File 2: domains of deprivation
url location:

https://www.gov.uk/government/statistics/english-indices-of-deprivation-2019

2019 indices containing individual metrics including health, education

Index of Multiple Deprivation (IMD) Decile (where 1 is most deprived 10% of LSOAs)

IMD Rank (1 is most deprived)

2. 2001 to 2018 edition of this dataset

Public houses and bars by local authority

url location:

https://www.ons.gov.uk/businessindustryandtrade/business/activitysizeandlocation/datasets/publichousesandbarsbylocalauthority

Using Pubs size LA 2018 by local authority. Gives the number of pubs in UK by local

authority

3. 2020 edition of this dataset

UK business: activity, size and location

url location:

https://www.ons.gov.uk/businessindustryandtrade/business/activitysizeandlocation/datasets/ukbusinessactivitysizeandlocation

ukbusinessworkbook2020.csv by Retail, Transport_Storage_inc_postal,

Accommodation_food services, Education, Health, Arts_entertainment

recreation_other_services

4. Local Authority Districts 2019 boundaries

Local Authority Districts in the United Kingdom, as at 31 December 2019. The boundaries available are:

- (BUC) Ultra Generalised (500m) - clipped to the coastline (Mean High Water mark).

https://geoportal.statistics.gov.uk/datasets/local-authority-districts-december-2019-boundaries-uk-buc

We use this as COVID-19 cases data is based on 2019 LA boundaries

5. Local Authority District to Public Health England Centre to Public Health England Region (December 2019) Lookup in England

url:

https://geoportal.statistics.gov.uk/datasets/local-authority-district-to-public-health-england-centre-to-public-health-england-region-december-2019-lookup-in-england

6. Mid-2019: April 2019 local authority district codes edition of this dataset

Population estimate data

url:
https://www.ons.gov.uk/peoplepopulationandcommunity/populationandmigration/populationestimates/datasets/populationestimatesforukenglandandwalesscotlandandnorthernireland

Using the following sheets: MYE2 – Males, MYE2 – Females, MYE3

(migrationFlow), MYE2 – Persons (contains age population).

7. SchoolOpening

url:

https://www.gov.uk/government/publications/actions-for-schools-during-the-coronavirus-outbreak/guidance-for-full-opening-schools

https://www.bbc.co.uk/news/uk-51952314

Schools have remained open to some pupils since 23 March, welcoming more pupils

back from 1 June.

During model generation, the SchoolOpening index was linked to the main

dataset based on the weeks the school restriction policies were implemented and the

relative effects at each time period. Index definition: 3 = No restrictions; 1.5 = School

closing but remaining open to some pupils; 3 = Also used to represent school

reopening.

Unlike the LockdownScore indices, the SchoolOpening index already takes

into account of the effect that school closing typically occurs when the number of

cases or mortality is highest, by inversing scoring. Hence, in this case when varying

the SchoolOpening parameter during model configuration mode, this metric will not

have an inverse effect.

Note, the effects pertain only to the local authorities selected.

8. Number of monthly arrivals in tourist accommodation in Spain from August 2018
   to July 2020*

url:

https://www.statista.com/statistics/1130775/number-of-monthly-arrivals-short-stay-accommodation-in-spain/
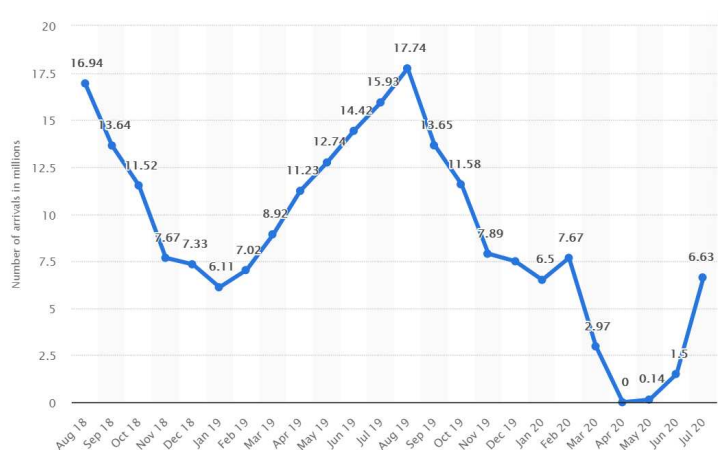
Figure S4.2. Monthly worldwide tourist arrivals in accommodation in Spain

We adjust tourist arrival by the proportion of UK citizens travelling to Spain in 2019

(section 9.)

Supplemental material

BMJ Publishing Group Limited (BMJ) disclaims all liability and responsibility arising from any reliance
placed on this supplemental material which has been supplied by the author(s)

BMJ Open
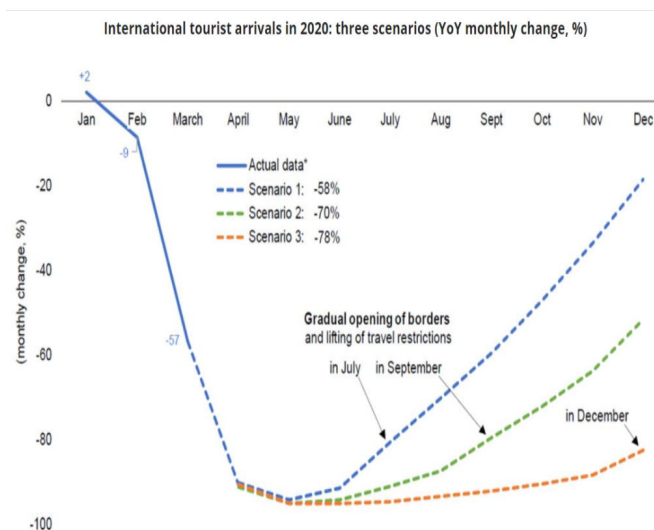
Figure S4.3 A reference model for understanding how quarantine measures are modelled.

url: https://www.adpr.co.uk/blog/covid-19/travel-and-tourism-brands-can-recover-from-coronavirus/

As UK removed 75 countries from quarantine list in July, we impute missing values from August to October based on the recovery model for July opening of borders above. However, the actual recovery based on the data is much faster than that shown in figure above.

9. Number of international tourists arriving in Spain in 2019, by country of residence

url:

https://www.statista.com/statistics/447683/foreign-tourists-visiting-spain-by-country-of-residence/

Obtains proportion of UK citizens arriving in Spain in 2019 as estimate for proportion in 2020

statistic_id447683_international-tourist-arrivals-in-spain-2019-by-country-of-residence.xlsx

UK proportion: 0.215984348

Supplemental material

BMJ Publishing Group Limited (BMJ) disclaims all liability and responsibility arising from any reliance placed on this supplemental material which has been supplied by the author(s)

BMJ Open

This is the estimated number of tourists arriving in Spain from UK in millions. The values are calculated based on number of tourists from various countries arriving in Spain from Jan 2020 to July 2020 and then adjusting by multiplying this number by the proportion of UK tourists in Spain from the preceding year i.e. 2019.

The weeks not covered by the data available i.e. August to October are imputed based on the tourism industry recovery model for July opening of borders https://www.adpr.co.uk/blog/covid-19/travel-and-tourism-brands-can-recover-from-coronavirus/.

This metric should be used as a guidance for how the situation will vary when international travel is restricted.

10. Public Health England Centres (December 2016) Ultra Generalised Clipped Boundaries in England

url:

https://geoportal.statistics.gov.uk/datasets/public-health-england-centres-december-2016-ultra-generalised-clipped-boundaries-in-england

2016 is the latest available

11. QuarantineMeasures

url:

https://www.theweek.co.uk/107044/UK-coronavirus-timeline+&cd=4&hl=en&ct=clnk&gl=uk

During model generation, the QuarantineMeasures index were linked to the main dataset based on the weeks the travel quarantine policies were implemented and the relative effects at each time period. Index definition: 1 = No quarantine; 10 = full quarantine of tourist from all countries; 5 = Removal of 59 countries from quarantine

list; 5.5 = Adding Spain back to the quarantine list following removal of 59 countries from the list.

As the level of travel quarantine restrictions implemented is dependent on the severity of covid-19 situation in other countries rather than the number of cases and mortality in UK, when varying this parameter during model configuration mode, this metric will have not an inverse effect.

Note, the effects pertain only to the local authorities selected.

12. LockdownScore

During model generation, the LockdownScore index were linked to the main dataset based on the weeks the lockdown policies were implemented and the relative effects at each time period. Index definition: 1 = No lock down; 4 = Local lock down; 5 = Local lock down with social distancing; 10 = Full Lock Down.

However, as the level of lock down implemented is typically highest when the number of cases or mortality is highest, when varying this parameter during model configuration mode, this metric will have an inverse effect. That is, changing the LockdownScore value to 1 will result in a full lock down, whilst changing to 10 will result in no lock down. 4 will result in Local lock down with social distancing and 5 will represent Local lock down.

Note, the effects pertain only to the local authorities selected.

Part II. B
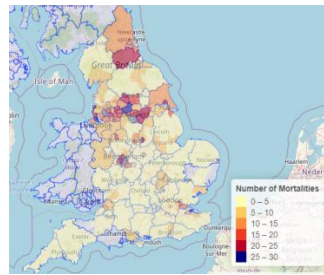
(i) M: Actual Mortalities Wk 46
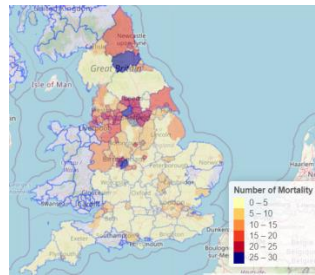
(ii) M: Wk 51 Local LD_SD
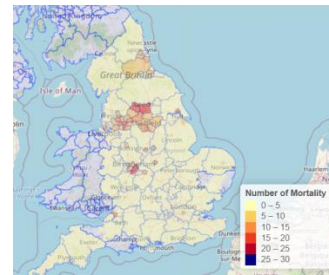
(iii) M: Wk 51 FLD
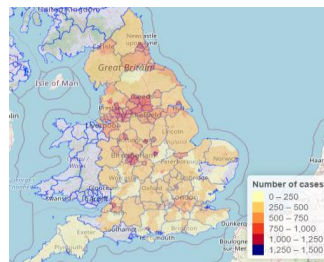
(iv) C: LD_SD -50% school
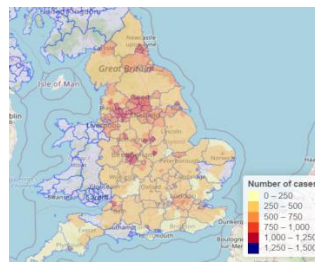
(v) C: LD_SD -50% food & accom
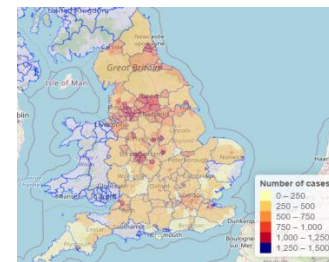
(vi) C: LD_SD -50% retail
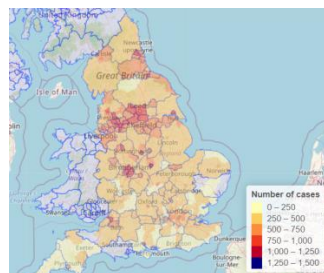
(vii) C: LD_SD -50% pubs
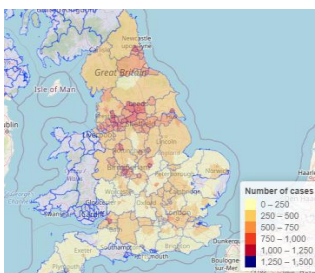
(viii) C: LD_SD intl travel -50%
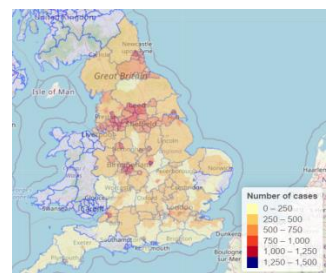
(ix) C: LD_SD 100% quarantine

Figure S5. Geographical level of cases and mortality for actual and predicted results based on different measures. C: cases; M: mortalities.

Supplemental material

BMJ Publishing Group Limited (BMJ) disclaims all liability and responsibility arising from any reliance placed on this supplemental material which has been supplied by the author(s)

BMJ Open

Part III

Table S2. Internal and external validation metrics for NCGFS compared against models from other studies.

Models	Predicted variables	RMSE	MAE	MAPE	Correlation Coefficient
Internal validation (week 46 FLD)					
NCGFS (England)	Cases	152.24	80.47	0.3649	0.81
Devaraj et al. SLSTM (India)	Cases	274.22	920.02	0.3	1.00
Melin et al. MNNF (Mexico)	Cases	1554.03	-	-	-
NCGFS (England)	Mortality	4.70	2.72	NaN*	0.76
Devaraj et al. SLSTM (India)	Mortality	309.12	278.29	0.6	1.00
Melin et al. MNNF (Mexico)	Mortality	170.00	-	-	-
External validation (week 51 LD_SD)					
NCGFS (21 hotspots)	Cases	798.83	721.42	1.23	0.27
NCGFS (21 hotspots)	Mortality	11.94	8.84	0.53	0.46
External validation (week 51 FLD)					
NCGFS (21 hotspots)	Cases	700.88	453.05	0.46	0.42
NCGFS (21 hotspots)	Mortality	14.91	10.05	0.39	0.68

* it was not possible to calculate MAPE here due to low LA rates and presence of zeros.

Table S3. Ranking of model compared to those from Devaraj et al.[3]

Model	Average Ranking	Overall Rank
NCGFS (England internal validation)	0.570	1
NCGFS (21 hotspots external validation FLD)	0.996	2
NCGFS (21 hotspots external validation LD_SD)	1.206	3
Devaraj et al. SLSTM (India)	1.753	4
Devaraj et al. ARIMA (India)	1.910	5
Devaraj et al. LSTM (India)	2.113	6

Part IV.

The deep learning model was used to generate the plots for fig S5. of the effects on

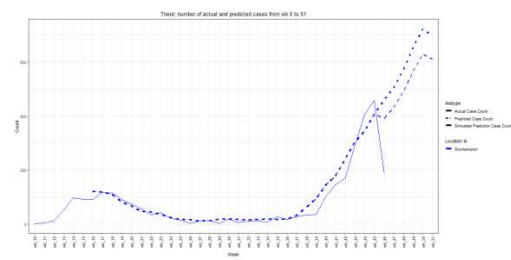the predicted number of cases for Southampton based on different measures.
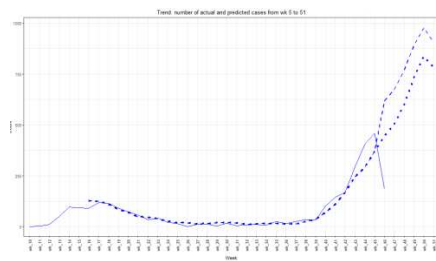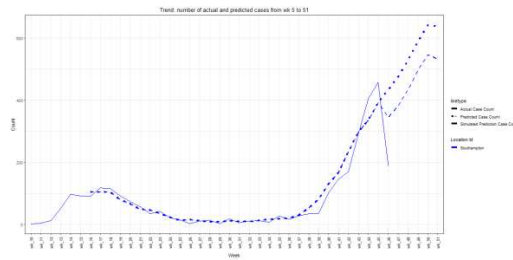

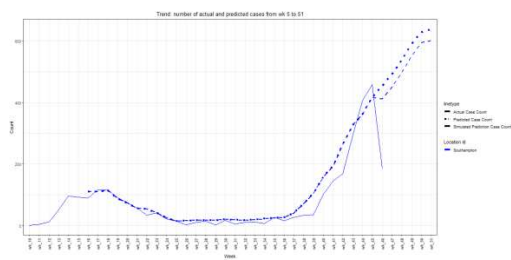(a) No lockdown vs. LD_SD
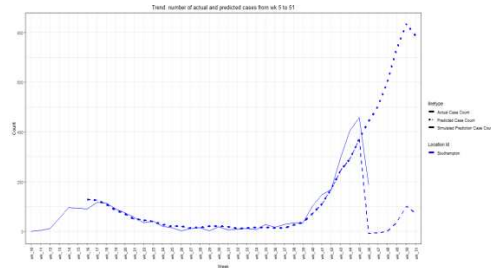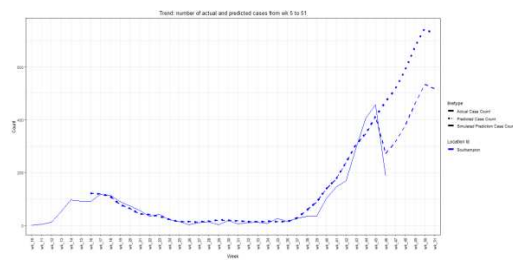
(b) LD_SD vs. full lockdown

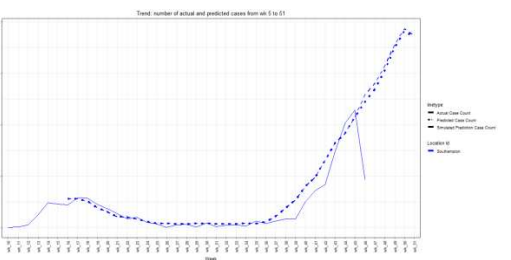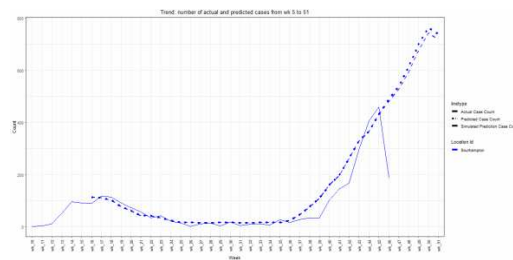(c) LD_SD vs. international travel -50%

(d) LD_SD vs. closing school -50%
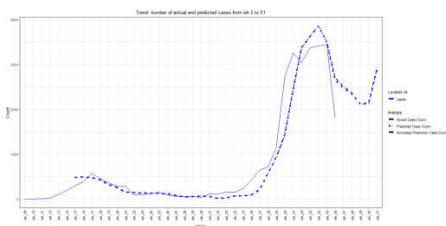
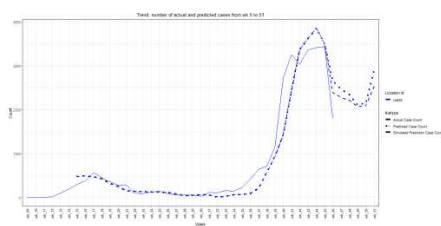(e) LD_SD (quarantine 5.5) vs. full quarantine (10) (f) LD_SD (100% pubs) vs. -50% pubs

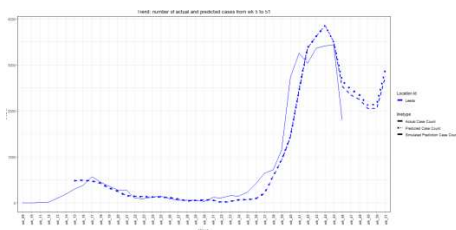(g) LD_SD (100% food & Accom) vs. -50%   (h) LD_SD (100% Retail) vs. -50% Retail

Figure S6. Cases forecast for Southampton by measure. The dotted line represents predictions using the LD_SD measures. The dashed lines represent prediction changes based on changes to measures. (c-h) relate to LD_SD without (left) and with (right) the supplementary measures.
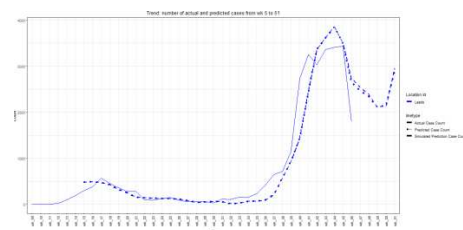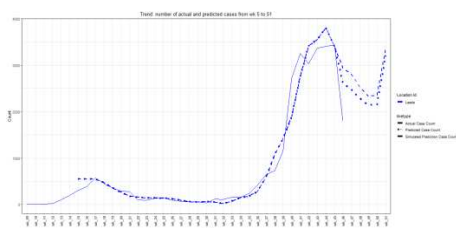

(a) No lockdown vs. LD_SD   (b) LD_SD vs. full lockdown
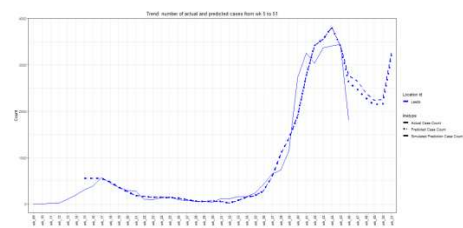

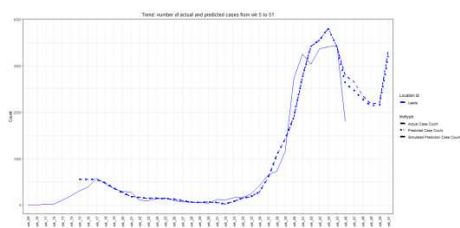(c) LD_SD vs. international travel -50%   (d) LD_SD vs. closing school -50%
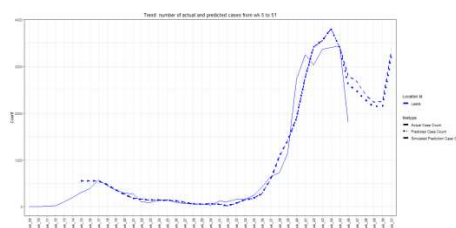

(e) LD_SD (quarantine 5.5) vs. full quarantine (10)   (f) LD_SD (100% pubs) vs. -50% pubs

(g) LD_SD (100% food & Accom) vs. -50%   (h) LD_SD (100% Retail) vs. -50% Retail

Figure S7. Cases forecast for Leeds by measures. The dotted line represents predictions using the LD_SD measures. The dashed lines represent prediction changes based on changes to measures. (c-h) relate to LD_SD without (left) and with (right) the supplementary measures.

References

1 Mnih V, Kavukcuoglu K, Silver D, *et al.* Human-level control through deep reinforcement learning. *Nature* 2015;**518**:529–33. doi:10.1038/nature14236

2 Sun S, Cao Z, Zhu H, *et al.* A Survey of Optimization Methods from a Machine Learning Perspective. *ArXiv190606821 Cs Math Stat* Published Online First: 23 October 2019.http://arxiv.org/abs/1906.06821 (accessed 24 Nov 2021).

3 Devaraj J, Madurai Elavarasan R, Pugazhendhi R, *et al.* Forecasting of COVID-19 cases using deep learning models: Is it reliable and practically significant? *Results Phys* 2021;**21**:103817. doi:10.1016/j.rinp.2021.103817